

Influence of fiber aspect ratio and orientation on the dielectric properties of polymer-based nanocomposites

Ricardo Simoes · Jaime Silva ·
Senentxu Lanceros-Mendez · Richard Vaia

Received: 25 June 2009 / Accepted: 30 September 2009 / Published online: 10 October 2009
© Springer Science+Business Media, LLC 2009

The addition of carbon nanotubes (CNT) to a polymeric matrix affects its mechanical and electrical properties. The changes can be significant even at small volume fractions of the reinforcement. The electrical properties are particularly sensitive to the CNT concentration. It is believed that the origin of this effect is the formation of a network of highly conductive CNTs forming preferential pathways for the electrical current to flow through. The CNT concentration, aspect ratio (AR), and dispersion are expected to affect the material response [1–4]. Because of the complexity of the problem and the lack of fundamental understanding on the underlying phenomena, computer simulations can provide useful insights.

The focus in the past years has been on statistical models to determine the percolation threshold. The percolation threshold or the concentration where an infinite cluster appears [5] can be predicted for high aspect ratio fillers in the framework of the excluded volume theory. In

general, the percolation threshold is defined within the following bounds:

$$1 - e^{-\frac{1.4V}{\langle V_e \rangle}} \leq \Phi_c \leq 1 - e^{-\frac{2.8V}{\langle V_e \rangle}} \quad (1)$$

Eq. 1, links the average excluded volume, $\langle V_e \rangle$, the volume around an object in which the center of another similarly shaped object is not allowed to penetrate averaged over the orientation distribution and the critical concentration (Φ_c). Here, the value 1.4 corresponds to the lower limit—infinitely thin cylinders—and the value 2.8 corresponds to spheres. The derivation of this equation and related discussion have been presented in [6]. With respect to the percolation threshold of high aspect ratio fillers it is also worth to mention the statistical work of Munson-McGee [7]. Berhan et al. [8, 9] also studied the percolation threshold of high aspect ratio fillers using soft-core and hard-core models. They draw two important conclusions that gave further confidence to the applicability of the excluded volume concept: that the hard-core approach is more appropriate for modeling electrical percolation onset in nanotube-reinforced composites and other high-aspect-ratio fiber systems, and that for high aspect-ratio fibers, the generally accepted inverse proportionality between percolation threshold and excluded volume holds, independent of fiber waviness.

The influence of the aspect ratio on the electrical properties of nanocomposites has been addressed in a recent experimental article by Sheng-Hong et al. [10]. They studied the electrical properties of poly(vinylidene fluoride) (PVDF)/Multi wall carbon nanotubes (MWCNT) composites. It was found that increasing aspect ratio increases the dielectric constant and the percolation threshold of the composite. The increase of the percolation threshold with the aspect ratio deviates from the predictions using the excluded volume theory. These authors explained this deviation with the formation of agglomerates which reduced

R. Simoes (✉) · J. Silva
IPC-Institute for Polymers and Composites, University
of Minho, Campus de Azurém, 4800-058 Guimarães, Portugal
e-mail: rsimoes@dep.uminho.pt

R. Simoes
Polytechnic Institute of Cávado and Ave, Campus do IPCA,
4750-810 Barcelos, Portugal
e-mail: rsimoes@ipca.pt

J. Silva · S. Lanceros-Mendez
Department of Physics, University of Minho, Campus
de Gualtar, 4710-057 Braga, Portugal

R. Vaia
Air Force Research Laboratories, Wright-Patterson Air Force
Base, Dayton, OH 45433-7750, USA

the fillers effective aspect ratio, increasing the percolation threshold.

The increase of the dielectric constant with filler volume fraction can be understood within the framework of the percolation theory [5]. The behavior of the conductivity and the dielectric constant at the composite critical concentration was studied earlier by Bergman and Imry [11] for heterogeneous mixtures of a conducting phase and an insulating matrix. An important result in this work is the divergence at the percolation threshold. The theoretical prediction was later completed in subsequent works by Stroud and Bergman [12].

A recent review in carbon fiber composites also addresses the problem of the wide range of critical concentrations values for the same type of filler/polymer composites [13] and the critical exponent s .

The effect of the alignment on the conductivity has been studied both numerically [14] and experimentally [15]. Experimental and numerical results demonstrate that as the anisotropy increases, for a fixed concentration, there is a critical value for the axial orientation parameter ($s = (3\langle \cos^2 \theta \rangle - 1)/2$), where s varies from 0 to 1 for isotropically and anisotropically oriented fibers, respectively. The same authors also observed a critical value for the axial orientation parameter (s_c) and, after that, a decrease in the conductivity.

In our previous work [16], a numerical procedure was developed enabling the calculation of the composite dielectric constant, dielectric strength, and voltage breakdown. The numerical results have been validated against experimental results. In yet earlier work, we had employed molecular dynamics simulations to study the structure-properties relationships driving the mechanical properties of polymer-based materials [17, 18]. That work included analysis of the true stress development in amorphous polymers, and the effect of loading conditions on deformation and creep.

In this letter we discuss the influence of the aspect ratio and the orientation of the nanotubes on the dielectric constant of polymer nanocomposites. In order to do this, isotropic and nematic materials were generated. As described in [16], the microstructure is generated by placing randomly oriented cylinders with an aspect ratio of 50 and 10 with a derivation of a sequential packing algorithm [19] for the isotropic materials. For the nematic state materials we constrain the zenith angle between 0 and 20° and randomly place the cylinders in domains; see Fig. 1. A minimum separation threshold of 1.0 nm was also defined with the purpose of avoiding quantum tunnelling effects. The threshold value is based on predictions of the order of the tunneling distance as 1 nm [20]. For each concentration, 10 different materials were generated with the same basic parameters, and then their final properties averaged.

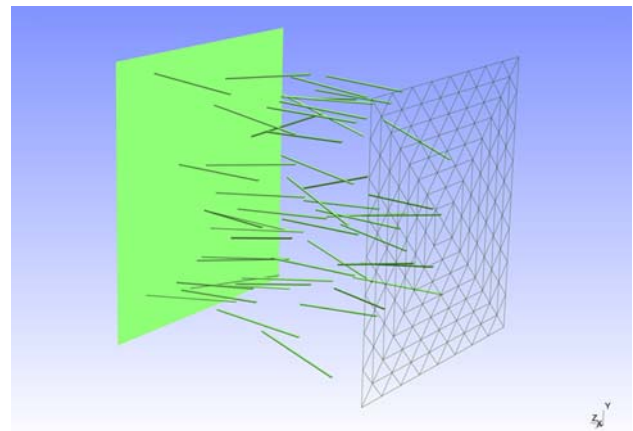


Fig. 1 Representation of a nematic material with an aspect ratio of 50

The properties of the dielectric matrix were kept constant in all cases; a dielectric constant value of 7 was chosen, from that of α -PVDF. The model was tested for consistency, proving that the values of the dielectric constant are independent of the number of particles in the box. For example, calculations for $\Phi = 5E-3$ in the cases of $N = 66$ and $N = 100$, revealed 16% deviation on average.

In Fig. 2 the results for the dielectric constant of random and nematic materials are shown. From the error bars, it is concluded that the standard error is higher for the random materials. This is related to the effect of the minimum distance and the rotation angle on the local capacitance [16]. For the anisotropic materials, a decrease of the standard error is observed due to the orientation of the cylinders. Also, based in Fig. 2, it can be concluded that: (a) increasing the aspect ratio will increase the dielectric constant (in agreement with recent experimental results for

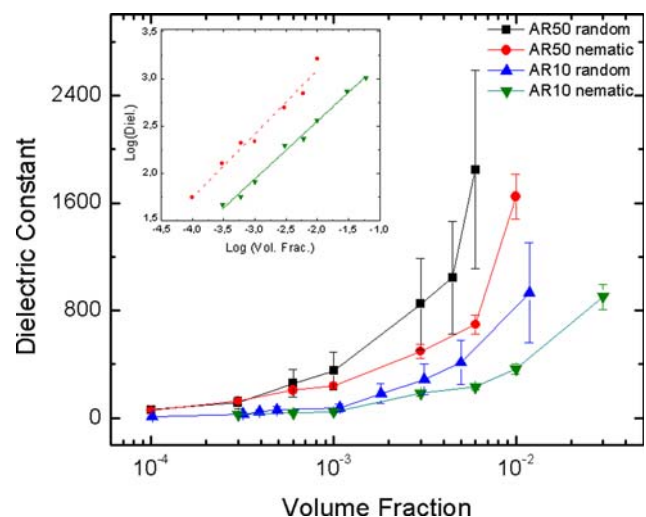


Fig. 2 Results for random and nematic materials with different aspect ratios (AR 10 and AR 50). In the inset the log–log plot for the nematic materials

the MWCNT/PVDF composites [10]; (b) nematic materials have a lower dielectric constant compared to isotropic ones. This result supports the ones previously obtained for the electrical conductivity [15].

The fact that nematic materials show a lower dielectric constant than isotropic ones (Fig. 2) is related to the zenith angle. It was demonstrated in [16] that parallel cylinders exhibit a lower capacitance, so the lower value for the composite dielectric constant is related to the filler alignment. It should be noted that in our simulations all the fillers are interacting with each other, removing the effect of different network topologies on the results, i.e., the number of serial or parallel capacitors in the network is the same for each material.

Using the results in Fig. 2 a power law can be fitted for the two nematic materials (AR 10 and AR 50). For the nematic AR 50 material, a linear fit in a log–log plot has a slope of 0.67 ± 0.48 and an intercept value of 4.43 ± 0.15 . For the nematic AR 10 materials the slope is 0.61 ± 0.48 and the intercept 3.77 ± 0.56 . The adjusted *R*-square for nematic AR 50 and AR 10 was 0.97 and 0.99. The later values indicate that the dielectric constant follows a power law:

$$\varepsilon(\Phi) = a\Phi^b \quad (2)$$

In Fig. 2inset, the log–log plots for the two types of nematic materials are shown. The *b* exponent should ideally have a lower deviation in order for us to try to relate the *b* values to physical features of the material, such as the dispersion. In any case, the *b* exponent values found for the two ARs are fairly similar excluding any relation with the filler aspect ratio.

The obtained power laws (Eq. 2) for the dielectric constant can be compared to similar ones previously obtained by Hu et al. [21] for the conductivity (Eq. 16 in the later article). Hu et al. [21] included a dependence on the aspect ratio in the percolation equation for straight CNTs, namely in the scaling constant. From the power laws calculated from our results, it can be seen that the *a* constant for AR 10 is 4.56 times greater than that of AR 50 one, so the *a* constant is related with filler aspect ratio, supporting the results of [21], in the limit of $\Phi_c \rightarrow 0$. Also by dividing the *a* constant by a suitable factor we can empirically find the results for lower AR using the calculated power laws.

This type of behavior, the continuous increase of the dielectric constant, is observed in several experimental results [22–24] and is related to the formation of a capacitive network where the long range Columbic interactions prevail [16]. Similar trends have also been found in related experimental work for MWCNT/PVDF composites [25].

In summary, it was found that an increase of the aspect ratio of the fillers increases the dielectric constant of the nanocomposite for the same volume fraction—supporting

recent experimental results for the dielectric constant in nanocomposites [10]. The nematic materials show a lower dielectric constant compared to isotropic ones—the same behavior had previously been found experimentally for the electrical conductivity [15]. It was also demonstrated that for nematic state materials with different aspect ratios, the dielectric constant follows a power law. The difference in the aspect ratios is reproduced in the power law scaling constant. Also, the power law exponent remains unchanged suggesting that it is related with the filler distribution and degree of anisotropy.

Acknowledgements Effort sponsored by the Air Force Office of Scientific Research, Air Force Material Command, USAF, under grant number FA8655-06-1-3009. The U.S Government is authorized to reproduce and distribute reprints for Governmental purpose notwithstanding any copyright notation thereon. We acknowledge also the Foundation for Science and Technology, Lisbon, through the 3° Quadro Comunitario de Apoio, the POCTI and FEDER programs, and the PTDC/CTM/69316/2006 grant.

References

1. Thostenson ET, Li C, Chou T-W (2005) *Compos Sci Technol* 65:491
2. Brostow W, Deborde JL, Jaclewicz M, Olzynski P (2003) *J Mater Educ* 25:119
3. Kopczyńska A, Ehrenstein WG (2007) *J Mater Educ* 29:325
4. Moniruzzaman M, Winey KI (2006) *Macromolecules* 39:5194
5. Stauffer D, Aharony A (1992) *An introduction to percolation theory*. Taylor and Francis, London
6. Celzard A, McRae E, Deleuze C, Dufort M, Furdin G, Marêché JF (1996) *Phys Rev B* 53:6209
7. Munson-McGee SH (1991) *Phys Rev B* 43:3331
8. Berhan L, Sastry AM (2007) *Phys Rev E* 75:041120
9. Berhan L, Sastry AM (2007) *Phys Rev E* 75:041121
10. Yao S-H, Dang Z-M, Jiang M-J, Xu H-P, Bai J (2007) *Appl Phys Lett* 91:212901
11. Bergman DJ, Imry Y (1977) *Phys Rev Lett* 39:1222
12. Stroud D, Bergman DJ (1982) *Phys Rev B* 25:2061
13. Al-Saleha MH, Sundarara U (2009) *Carbon* 47:2
14. White SI, DiDonna BA, Mu M, Lubensky TC, Winey KI (2009) *Phys Rev B* 79:024301
15. Du F, Fischer JE, Winey KI (2005) *Phys Rev B* 72:121404
16. Simoes R, Silva J, Vaia R, Sencadas V, Costa P, Gomes J, Lanceros-Mendez S (2009) *Nanotechnology* 20:035703
17. Simões R, Cunha AM, Brostow W (2006) *Comp Mater Sci* 36:319
18. Simoes R, Cunha AM, Brostow W (2006) *Model Simul Mater Sci Eng* 14:157
19. Vold MJ (1959) *J Phys Chem-US* 63:1608
20. Balberg I (1987) *Phys Rev Lett* 59:1305
21. Ning H, Masuda Z, Cheng Y, Yamamoto G (2008) *Nanotechnology* 19:215701
22. Mdarhri A, Carmona F, Brosseau C, Delhaes P (2008) *J Appl Phys* 103:054303
23. Ahmad K, Pan W, Shi S-L (2006) *Appl Phys Lett* 89:133122
24. Zhu B-K, Xie S-H, Xu Z-K, Xu Y-Y (2006) *Compos Sci Technol* 66:548
25. Dang Z-M, Wang L, Yin Y, Zhang Q, Lei Q-Q (2007) *Adv Mater* 19:852